

**Polarized Raman spectroscopy of nearly tetragonal BiFeO<sub>3</sub> thin films**

M. N. Iliev

*Texas Center for Superconductivity and Department of Physics, University of Houston, Houston, Texas 77204-5002, USA*

M. V. Abrashev

*Faculty of Physics, University of Sofia, 1164 Sofia, Bulgaria*

D. Mazumdar, V. Shelke, and A. Gupta

*Center for Materials for Information Technology, University of Alabama, Tuscaloosa, Alabama 35487, USA*

(Received 16 April 2010; revised manuscript received 18 May 2010; published 12 July 2010)

BiFeO<sub>3</sub> thin films can be epitaxially stabilized in a nearly tetragonal phase under a high biaxial compressive strain. Here we investigate the polarized Raman spectra of constrained BiFeO<sub>3</sub> films with tetragonal-like (BFO-T), rhombohedral-like (BFO-R), and multiphase (BFO-T+R) structure. Based on analysis of the number and symmetry of the Raman lines, we provide strong experimental evidence that the nearly tetragonal films are monoclinic (*Cc* symmetry) and not tetragonal (*P4mm*). Through the Raman mapping technique we show localized coexistence of BFO-T and BFO-R phases with the relative fraction dependent on the film thickness.

DOI: [10.1103/PhysRevB.82.014107](https://doi.org/10.1103/PhysRevB.82.014107)

PACS number(s): 78.30.-j, 63.22.-m, 75.85.+t

**I. INTRODUCTION**

Constant demand for miniaturization in modern devices has provided a big stimulus for research into multifunctional materials. BiFeO<sub>3</sub>, or simply BFO, is a prototypical multiferroic material due to the simultaneous coexistence of ferroelectric, ferroelastic, and antiferromagnetic order. It is also currently widely investigated as it offers room-temperature multifunctionality after very high-polarization values were reported in 2003 for films grown on SrTiO<sub>3</sub> (STO) substrates.<sup>1</sup> However, it can be argued that the rhombohedral *R3c* structure of BFO with rhombohedral-like (BFO-R) possess significant difficulties and challenges. For example, the ferroelectric polarization of BFO-R is directed along the [111] direction giving rise to eight possible polarization orientations. As a result, ferroelectric switching is complicated and difficult to control for any meaningful multifunctionality. Therefore, BFO phase of different symmetry, which, in principle, could address these issues, is desired.

This interest increased after it was recently predicted theoretically and confirmed experimentally that the structure and properties of BiFeO<sub>3</sub> films under a large, biaxial compressive strain could deviate significantly from the bulk material into a “supertetragonal” structure with an extremely high *c/a* ratio.<sup>2-7</sup> This phase, in some sense, appears incommensurable to its rhombohedral counterpart and requires a thorough investigation, much along the lines that bulk BFO has received. Apart from possibly higher ferroelectric polarization values and significantly simpler switching properties, this phase is especially suitable for ultrathin-film applications where the strain effect is maximum.

Following predictions of desirable properties in hypothetical *P4mm* BFO a number of groups searched for the structure in strained thin films but careful x-ray diffraction analysis of BFO films deposited on LaAlO<sub>3</sub> (LAO) and YAlO<sub>3</sub> substrates shows evidence of monoclinic distortions,<sup>5,6</sup> and very recently *ab initio* calculations have also indicated<sup>7</sup> that the monoclinic *Cc* (No. 9) structure is indeed energetically more favorable than the tetragonal *P4mm* structure, when the

compressive strain is greater than 4%. The three structures that could be used to describe strained BFO thin films grown on LAO substrates are shown in Fig. 1. Following the theoretical study of Hatt *et al.*,<sup>7</sup> only small differences from the structure of the bulk material are predicted and observed at low strain. Although the strained film is of lower monoclinic symmetry (*Cc*), its structure remains rhombohedral-like and to a good approximation can be described by the *R3c* space group. For compressive strains greater than 4% the structure changes dramatically and becomes tetragonal-like with *c/a* ≈ 1.2–1.3. This structure can be approximated by the *P4mm* symmetry, but further refinement, supported by first-principles calculations, leads again to *Cc* symmetry. As pointed out in Refs. 6 and 7, the strain induced R-T transition of BiFeO<sub>3</sub> is in fact isosymmetric. Although theoretically well grounded and supported by x-ray experiments,<sup>5,6</sup> there is to our knowledge no other reports of direct experimental confirmation that at a local level the structure of BFO-T films is monoclinic. Strong experimental evidence for *Cc* structure of BFO with tetragonal-like (BFO-T) films has been readily found in the polarized Raman spectra presented and discussed below.

There are several reports on the Raman spectra of BiFeO<sub>3</sub> obtained from single crystal,<sup>8-11</sup> polycrystalline samples,<sup>12,13</sup> and thin films on SrTiO<sub>3</sub> substrates.<sup>10,14-16</sup> These spectra are

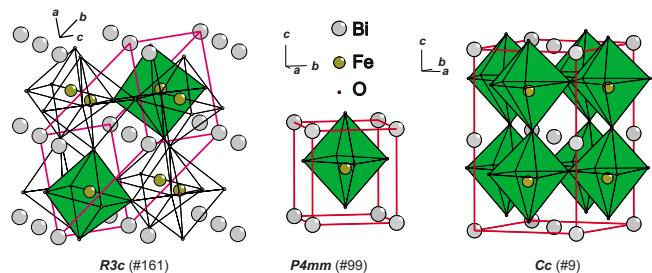


FIG. 1. (Color online) Elementary cells of the rhombohedral (*R3c*), tetragonal (*P4mm*), and tetragonal-like (*Cc*) structures used to describe strained BFO/LAO films.

TABLE I. Polarization selection rules for the phonons of nonzero intensity with backward scattering from the  $(001)_c$  plane of  $R3c$ ,  $(001)_r=(001)_c$  plane of  $P4mm$ , or  $(001)_m$  plane of  $Cc$  structures. The intensities for  $R3c$  and  $Cc$  modes are averaged over the expected twin variants.

Mode	$(xx)_c$ $(xx)_r$ $(x'x')_m$	$(yy)_c$ $(yy)_r$ $(y'y')_m$	$(xy)_c$ $(xy)_r$ $(x'y')_m$	$(x'x')_c$ $(x'x')_r$ $(xx)_m$	$(y'y')_c$ $(y'y')_r$ $(yy)_m$	$(x'y')_c$ $(x'y')_r$ $(xy)_m$
$A_1(R3c)$	$\frac{1}{9}(2a+b)^2$	$\frac{1}{9}(2a+b)^2$	$\frac{1}{9}(a-b)^2 \approx 0$	$\frac{1}{2}[a^2 + \frac{1}{9}(a+2b)^2]$	$\frac{1}{2}[a^2 + \frac{1}{9}(a+2b)^2]$	0
$E(R3c)$	$\frac{4}{9}(-c + \sqrt{2}d)^2$	$\frac{4}{9}(-c + \sqrt{2}d)^2$	$\frac{1}{9}(2c + \sqrt{2}d)^2$	$\frac{1}{2}[c^2 + \frac{1}{9}(c + 2\sqrt{2}d)^2]$	$\frac{1}{2}[c^2 + \frac{1}{9}(c + 2\sqrt{2}d)^2]$	$\frac{1}{3}(-c + \sqrt{2}d)^2$
$A_1(4mm)$	$a^2$	$a^2$	0	$a^2$	$a^2$	0
$B_1(4mm)$	$c^2$	$c^2$	0	0	0	$c^2$
$A'(Cc)$	$\frac{1}{4}(a+b)^2$	$\frac{1}{4}(a+b)^2$	$\frac{1}{4}(a-b)^2 \approx 0$	$\frac{1}{2}(a^2 + b^2)$	$\frac{1}{2}(a^2 + b^2)$	0
$A''(Cc)$	$e^2$	$e^2$	0	0	0	$e^2$

similar with respect to the frequencies of the observed Raman lines and their assignment is based on the rhombohedral  $R3c$  structure. As an exception, Singh *et al.*<sup>14</sup> and Palai *et al.*<sup>10</sup> have assumed that the BFO/STO film they studied have, respectively, tetragonal  $P4mm$  and monoclinic  $Bb$  structure. However, the spectra of Refs. 10 and 14 are practically identical to those for strain-free rhombohedral  $\text{BiFeO}_3$ .<sup>8,9,12,13</sup> In addition, the type of substrate ( $\text{SrTiO}_3$ ) and the film thickness (600 and 300 nm) are favorable for growth of the rhombohedral-like structure.<sup>7</sup>

Here we report the polarized Raman spectra of true BFO-T obtained in strained 70 and 100 nm epitaxial  $\text{BiFeO}_3$  films on  $(001)$ - $\text{LaAlO}_3$  substrates. The spectra are compared to those of relaxed BFO-R 80 nm  $\text{BiFO}_3/40$  nm  $\text{SrRuO}_3/\text{LaAlO}_3$  films and mixed 200 nm  $\text{BiFO}_3/\text{LaAlO}_3$  films. Based on analysis of the number and symmetry of the Raman lines expected for the tetragonal  $P4mm$  and monoclinic  $Cc$  BFO structures, the experimental spectra provide strong evidence that the real structure is of  $Cc$  symmetry. We also show by Raman mapping of selected areas on the 100 nm BFO/LAO and 200 nm BFO/LAO films that BFT-T and BFO-R phases can coexist in partly relaxed BFO/LAO films.

## II. SAMPLES AND EXPERIMENTAL

$\text{BiFeO}_3$  thin films were deposited on single-crystal  $\text{LaAlO}_3$  substrates by pulsed-laser deposition using 248 nm, KrF excimer laser with 1.5 J/cm<sup>2</sup> fluence and 10 Hz pulse repetition rate. A ceramic target with 20% Bi excess was used to compensate the Bi loss during deposition. The substrate temperature of 700 °C, oxygen pressure 100 mTorr and cool down at 5 °C/min with 600 Torr oxygen pressure were used for all the depositions. Additionally, BFO films were deposited on 40 nm  $\text{SrRuO}_3$  (SRO) buffered LAO substrates. X-ray diffraction measurements show BFO films (70–200 nm) deposited directly on LAO substrates to have an out-of-plane lattice constant value of approximately 4.66 Å, whereas SRO-buffered films exhibit a diffraction peak near the bulk rhombohedral BFO position (pseudocubic  $c \approx 3.96$  Å).<sup>18</sup> In-plane lattice parameter measurements through reciprocal space maps show BFO/LAO films to be highly strained to the substrate ( $a \approx 3.79$  Å).

The Raman spectra were measured at room temperature using a triple Raman spectrometer T64000 equipped with microscope and computer-controlled XY stage. Both 515 nm and 488 nm laser lines were used for excitation, the spectra being practically identical. The spectra of air and the LAO substrate were measured separately and their contributions were subtracted from the original spectra.

## III. RAMAN PHONON MODES AND POLARIZATION SELECTION RULES

The  $R3c$  primitive cell contains two formula units. The total number of  $\Gamma$ -point phonon modes is 20 ( $5A_1 + 5A_2 + 10E$ ). Of these, 13 ( $4A_1 + 9E$ ) are both Raman and infrared (IR) active, five ( $5A_2$ ) are silent, and two ( $A_1 + E$ ) are acoustical modes. The primitive cell of the  $P4mm$  structure (Fig. 1) contains one formula unit. The total number of  $\Gamma$ -point phonon modes is 10 ( $4A_1 + B_1 + 5E$ ). Of these, seven ( $3A_1 + 4E$ ) are both Raman and IR active, one ( $B_1$ ) is only Raman active, and two ( $A_1 + E$ ) are acoustic modes. The elementary cell of  $Cc$  structure (Fig. 1) is base centered and contains four formula units. All atoms are at noncentrosymmetrical ( $4a$ ) positions. The number of  $\Gamma$ -point phonon modes is 30 ( $15A' + 15A''$ ). Three of them ( $A' + 2A''$ ) are acoustic modes.  $14A' + 13A''$  modes are both Raman and infrared active. As the experimentally obtained out-of-plane lattice parameter of the BFO-T films is larger than the in-plane parameters, it is plausible to accept that the surface of the film is parallel to the corresponding  $(001)$  planes. We note here that  $[100]_r$  and  $[010]_r$  directions of  $P4mm$  structure, which are parallel to  $[100]_c$  and  $[010]_c$  quasicubic directions of the LAO substrate, become  $[110]_m$  and  $[\bar{1}10]_m$  directions for the  $Cc$  structure. Therefore, the coordinate systems of the Raman tensors for the  $P4mm$  and  $Cc$  differ by 45° rotation around the  $c$  axis.

The scattering intensity of a phonon mode of given symmetry is proportional to  $(\vec{e}_i \mathbf{R} \vec{e}_s)^2$ , where  $\vec{e}_i$  and  $\vec{e}_s$  are unit vectors parallel, respectively, to the polarization of the incident and scattered radiation. The Raman tensors for modes of different symmetry of the  $R3c$ ,  $P4mm$ , and  $Cc$  structures have the form<sup>17</sup>

$$R3c \Rightarrow \begin{bmatrix} A_1 \\ a & a & b \end{bmatrix} \begin{bmatrix} c & d \\ -c & d \end{bmatrix}, \begin{bmatrix} E \\ -c & d \end{bmatrix},$$

$$P4mm \Rightarrow \begin{bmatrix} A_1 \\ a & a & b \end{bmatrix} \begin{bmatrix} B_1 \\ c & -c \end{bmatrix} \begin{bmatrix} E \\ e \end{bmatrix}, \begin{bmatrix} e \\ e \end{bmatrix},$$

and

$$Cc \Rightarrow \begin{bmatrix} A' \\ a & d \\ b & c \\ d & c \end{bmatrix} \begin{bmatrix} A'' \\ e & f \\ e & f \end{bmatrix}.$$

For backward scattering from the (001) surface,  $\vec{e}_i$  and  $\vec{e}_s$  have no  $z$  component and the intensity of the  $E$  modes (for  $P4mm$ ) will *a priori* be zero. One therefore expects observation in the experimental Raman spectra of BFO-T of only four ( $3A_1+B_1$ ) Raman lines in the case of  $P4mm$  and many more lines ( $14A'+13A''$ ) for the  $Cc$  structure. The polarization selection rules for these Raman mode symmetries in all available exact scattering configurations from the tetragonal (001)<sub>t</sub> or monoclinic (001)<sub>m</sub> surfaces are given in Table I. For the  $Cc$  structure the intensities are averaged over the expected two twin variants with interchangeable  $a$  and  $b$  parameters (four twin variants with accounting for the polarization direction). Similarly, for the BFO-R films four twin variants (eight with accounting for the polarization direction) with orientation of the rhombohedral  $[111]_r$  direction along any of the four quasicubic directions  $111_c$  of the LAO substrate may coexist. The polarization selection rules for the  $R3c$  and  $Cc$  structures, given in Table I, are the expected averaged Raman intensities with  $\vec{e}_i$  and  $\vec{e}_s$  along the cubic ( $x$ ,  $y$ ,  $x'$ , and  $y'$ ) directions, under the assumption that the twin variants occupy equal parts of the scattering volume.

#### IV. RESULTS AND DISCUSSION

Figure 2 illustrates by way of the example of 70 nm BFO/LAO film how the spectra of BFO-T were obtained. Due to the small film thickness, the original spectra are a superposition (BFO+LAO) of Raman signals from the film (BFO) and the substrate (LAO). The LAO spectra were measured separately with the same scattering configuration from film-free substrate surface and then subtracted from the original spectra using GRAMS AI software.

In Fig. 3 are compared the spectra of BFO-T, obtained with 515 and 488 nm excitation from two strained BFO-T films, with the corresponding spectra of relaxed BFO-R, obtained with 488 nm excitation. As it follows from Table I, the

$A_1$  modes of BRO-R structures are much stronger with parallel ( $xx/yy$ ) and ( $x'x'/y'y'$ ) than with crossed ( $xy$ ) and ( $x'y'$ ) scattering configurations. This allows to identify unambiguously the peaks at 77, 142, 176, and 221  $\text{cm}^{-1}$  in the BFO-R spectra as corresponding to the  $A_1$  modes. The assignment of the 77  $\text{cm}^{-1}$  line to an  $A_1$  mode differs from that proposed by Cazayous *et al.*,<sup>9</sup> but overall the BFO-R spectra are similar to those reported for single crystal and bulk

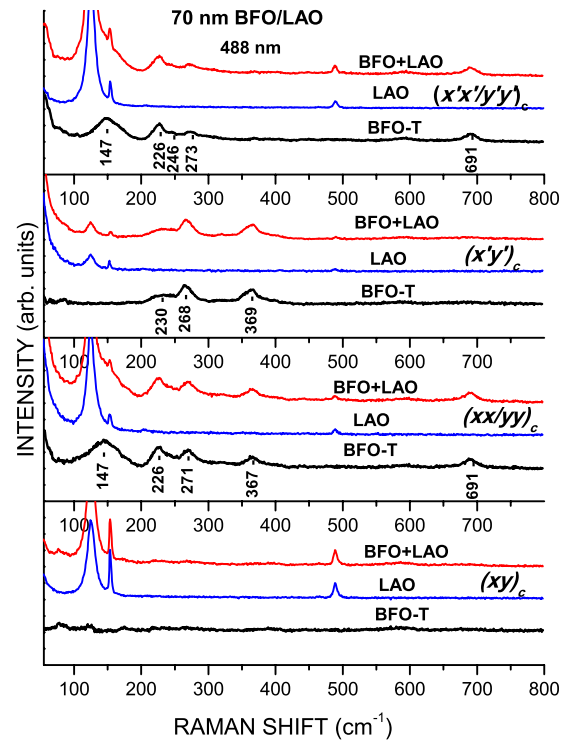


FIG. 2. (Color online) Polarized Raman spectra of BFO/LAO, LAO and extracted spectra of tetragonal-like BFO-T as obtained with 488 nm excitation from a 70 nm BFO/LAO film.

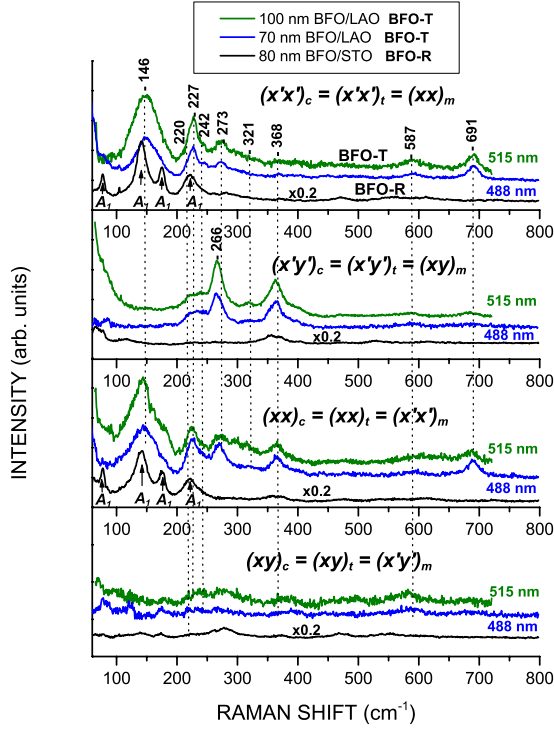


FIG. 3. (Color online) Comparison of the spectra of BFO-T obtained from 70 nm BFO/LAO and 100 nm BFO/LAO with the spectra of BFO-R obtained from a 80 nm BFO/STO/LAO thin film. The spectra with 488 nm excitation were obtained under the same experimental conditions. The spectra of BFO-R are scaled by a factor of 0.2.

BFO.<sup>8,9,12,13</sup> The weaker peaks at 279, 359, 369, 473, 530, and 615  $\text{cm}^{-1}$  can be assigned to  $E$  modes.

The Raman spectra of BFO-T are well reproduced in all scattering configurations. The large number of Raman lines is consistent with monoclinically distorted tetragonal-like  $Cc$  structure, thus ruling out the simple  $P4mm$  structure. Indeed, for the  $P4mm$  structure one expects only three  $A_1$  lines in the  $(x'x')_c$  and one  $B_1$  line in the  $(x'y')_c$  spectra, whereas the number of experimentally observed lines is much higher. For the same scattering configurations  $14A'$  and  $13A''$  modes are allowed, respectively, for the  $Cc$  structure. We can therefore assign the Raman lines at 146, 227, 273, 587, and 691  $\text{cm}^{-1}$ , pronounced in the  $(xx)_c$  ( $A'+A''$ ) and  $(x'x')_c$  ( $A'$ ) spectra, to modes of  $A'$  symmetry and the lines at 220, 242, 266, and 368  $\text{cm}^{-1}$ , seen in the  $(xx)_c$  ( $A'+A''$ ) and  $(x'y')_c$  ( $A''$ ) spectra, to modes of  $A''$  symmetry. It is worth mentioning that based on the Raman data it is not possible to differentiate between the  $Cc$  and alternatively suggested  $Cm$  structure.<sup>5</sup>

With increasing BFO/LAO film thickness the rhombohedral BFO-R phase appears as a secondary phase in the 100 nm BFO/LAO film and the dominant phase in the 200 nm BFO/LAO film.<sup>6,18</sup> This is illustrated for  $45 \times 45 \mu\text{m}^2$  area on the surface of 100 nm BFO/LAO thin film, which has been Raman mapped with 1.5  $\mu\text{m}$  steps, comparing the  $(xx)_c$  Raman spectra. As it follows from Fig. 4, the studied area is characterized by three types of spectra: BFO-R1, BFO-R2, and BFO-T. The Raman line frequencies of BFO-R1 and BFO-R2 correspond to the rhombohedral phase and the spec-

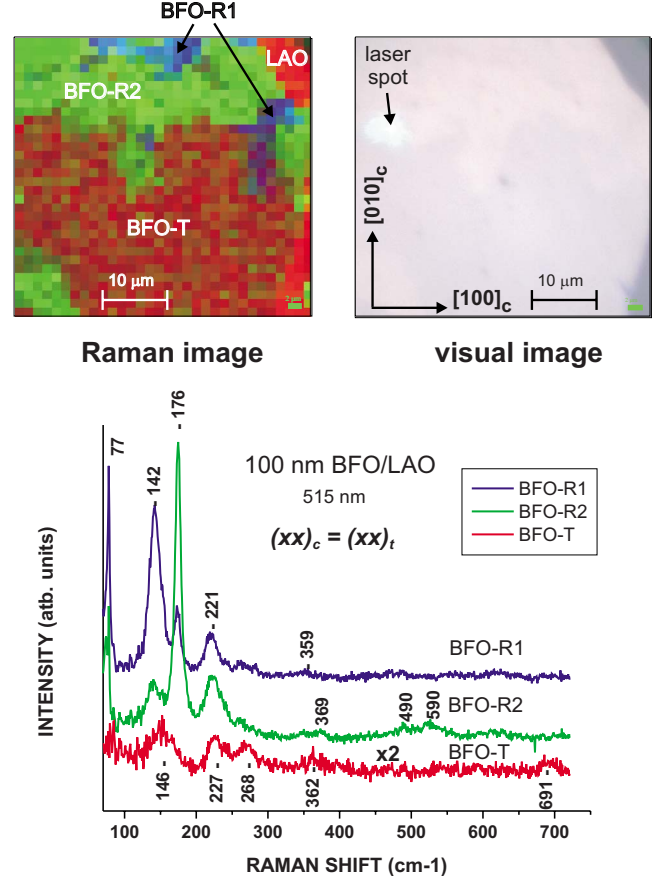


FIG. 4. (Color online) Raman mapping (upper left) and visual image (upper right) of the same  $45 \times 45 \mu\text{m}^2$  area on the surface of 100 nm BFO/LAO thin film. The blue and green colors indicate presence of BFO-R twin variants of different orientation. The red colored area corresponds to the BFO-T phase. In the bottom panel are shown the corresponding Raman spectra obtained with  $(xx)_c$  scattering configuration with 515 nm excitation.

tra differ only in the relative line intensities. This can be explained by assuming that BFO-R1 and BFO-R2 spectra are obtained from twin variants of BFO-R with different orientation with respect to  $\vec{e}_i$  and  $\vec{e}_s$ . One can therefore conclude that the twin variants of the BFO-R phase are of micrometer size. As to the twin variants of the BFO-T phase, their Raman spectra should be practically undistinguishable since from structural considerations one expects the relation  $a \approx b$  for the components of the  $A'$  Raman tensor. The observation of the R phase is likely due to the release of the substrate strain effect with increasing thickness.<sup>6</sup>

## V. CONCLUSIONS

In conclusion, polarized Raman spectroscopy has been used to study tetragonally strained BFO-T films on LAO substrates and relaxed rhombohedral BFO-R films on LAO substrates with SRO buffer layers. We provide strong experimental evidence that the tetragonal-like structure is of monoclinic  $Cc$  symmetry and the simple tetragonal  $P4mm$  structure can be ruled out. Five of the fourteen  $A'$  modes and four

of the thirteen  $A''$  modes expected for the  $Cc$  structure have been identified. This is consistent with the results of recent first-principles calculations.<sup>7</sup> We have also clearly demonstrated that BFO-R and BFO-T coexist at the micrometer scale, with the R phase gradually becoming the dominant phase with increasing film thickness.

## ACKNOWLEDGMENTS

This work was supported in part by the State of Texas through the Texas Center for Superconductivity at the University of Houston. The work at the University of Alabama was supported by ONR (Grant No. N00014-09-0119).

- 
- <sup>1</sup>J. Wang, J. B. Neaton, H. Zheng, V. Nagarajan, S. B. Ogale, B. Liu, D. Viehland, V. Vaithyanathan, D. G. Schlom, U. V. Waghmare, N. A. Spaldin, K. M. Rabe, M. Wuttig, and R. Ramesh, *Science* **299**, 1719 (2003).
- <sup>2</sup>C. Ederer and N. A. Spaldin, *Phys. Rev. Lett.* **95**, 257601 (2005).
- <sup>3</sup>K. Y. Yun, D. Ricinchi, T. Kanashima, and M. Okuyama, *Appl. Phys. Lett.* **89**, 192902 (2006).
- <sup>4</sup>S. Lisenkov, D. Rahmedov, and L. Bellaiche, *Phys. Rev. Lett.* **103**, 047204 (2009).
- <sup>5</sup>H. Béa, B. Dupé, S. Fusil, R. Mattana, E. Jacquet, B. Warot-Fonrose, F. Wilhelm, A. Rogalev, S. Petit, V. Cros, A. Anane, F. Petroff, K. Bouzehouane, G. Geneste, B. Dkhil, S. Lisenkov, I. Ponomareva, L. Bellaiche, M. Bibes, and A. Barthélémy, *Phys. Rev. Lett.* **102**, 217603 (2009).
- <sup>6</sup>R. J. Zeches, M. D. Rossell, J. X. Zhang, A. J. Hatt, Q. He, C.-H. Yang, A. Kumar, C. H. Wang, A. Melville, C. Adamo, G. Sheng, Y.-H. Chu, J. F. Ihlefeld, R. Erni, C. Ederer, V. Gopalan, L. Q. Chen, D. G. Schlom, N. A. Spaldin, L. W. Martin, and R. Ramesh, *Science* **326**, 977 (2009).
- <sup>7</sup>A. J. Hatt, N. A. Spaldin, and C. Ederer, *Phys. Rev. B* **81**, 054109 (2010).
- <sup>8</sup>H. Fukumura, S. Matsui, H. Harima, T. Takahashi, T. Itoh, K. Kisoda, M. Tamada, Y. Noguchi, and M. Miyavama, *J. Phys.: Condens. Matter* **19**, 365224 (2007).
- <sup>9</sup>M. Cazayous, D. Malka, D. Lebeugle, and D. Colson, *Appl. Phys. Lett.* **91**, 071910 (2007).
- <sup>10</sup>R. Palai, R. S. Katiyar, H. Schmid, P. Tissot, S. J. Clark, J. Robertson, S. A. T. Redfern, G. Catalan, and J. F. Scott, *Phys. Rev. B* **77**, 014110 (2008).
- <sup>11</sup>R. Palai, H. Schmid, J. F. Scott, and R. S. Katiyar, *Phys. Rev. B* **81**, 064110 (2010); for erratum see **81**, 139903(E) (2010).
- <sup>12</sup>G. L. Yuan, S. W. Or, and H. L. W. Chan, *J. Phys. D* **40**, 1196 (2007).
- <sup>13</sup>D. Rout, K.-S. Moon, and S.-J. L. Kang, *J. Raman Spectrosc.* **40**, 618 (2009).
- <sup>14</sup>M. K. Singh, S. Ryu, and H. M. Jang, *Phys. Rev. B* **72**, 132101 (2005).
- <sup>15</sup>Y. Yang, J. Y. Sun, K. Zhu, Y. L. Liu, and L. Wan, *J. Appl. Phys.* **103**, 093532 (2008).
- <sup>16</sup>R. Palai, J. F. Scott, and R. S. Katiyar, *Phys. Rev. B* **81**, 024115 (2010).
- <sup>17</sup>See, e.g., Bilbao Crystallographic Server, <http://www.cryst.ehu.es/rep/sam.html>
- <sup>18</sup>D. Mazumdar, V. Shelke, M. Iliev, S. Jesse, A. Kumar, S. Kalinin, A. Baddorf, and A. Gupta, *Nano Lett.* (to be published).